Research Journal of Biological Sciences 4 (9): 1032-1036, 2009
ISSN: 1815-8846

Synthesis and Antibacterial Activity of Silver/Montmorillonite Nanocomposites

[1]Mansor Bin Ahmad, [1]Kamyar Shameli, [2]Majid Darroudi, [1]Wan Md Zin Wan Yunus,
[1]Nor Azowa Ibrahim, [3]Azizah Abdul Hamid and [3]Mohsen Zargar
[1]Department of Chemistry, Faculty of Science, Putra Malaysia University,
43400 Serdang, Selangor, Malaysia
[2]Laboratory of Advanced Materials and Nanotechnology,
Institute of Advanced Technology (ITMA),
Putra Malaysia University, 43400 Serdang, Selangor, Malaysia
[3]Department of Food Science, Faculty of Food Science and Biotechnology,
Putra University Malaysia, 43400 Serdang, Selangor, Malaysia

Abstract: Silver nanoparticles (Ag-NPs) were successfully synthesized into the interlayer space of Montmorillonite (MMT) by chemical reduction method. $AgNO_3$ and $NaBH_4$ were used as a silver precursor and reducing agent, respectively. The properties of Ag/MMT nanocomposites were studied as a function of the $AgNO_3$ concentration. The UV-vis spectra of synthesized Ag-NPs showed that the intensity of the maximum wavelength of the plasmon peaks increased with increasing $AgNO_3$ concentration. The crystalline structure of the Ag-NPs and basal spacing of MMT and Ag/MMT were also studied by Powder X-Ray Diffraction (PXRD). The antibacterial activity of Ag-NPs was investigated against gram-negative bacteria (*Escherichia coli*, *Escherichia coli* O157:H7 and *K. pneumonia*) and gram-positive bacterium (*Staphylococcus aureus*) by disk diffusion method using Muller-Hinton Agar (MHA) at different sizes of Ag-NPs. The smaller Ag-NPs were found to have significantly higher antibacterial activity. These results showed that Ag-NPs can be used as effective growth inhibitors in different biological systems, making them applicable to medical applications such as in surgical devices.

Key words: Silver nanoparticles, montmorillonite, nanocomposite, antibacterial activity, powder x-ray diffraction, muller-hinton agar

INTRODUCTION

The investigation on the antibacterial Activity of silver Nanoparticles (Ag-NPs) has regained importance due to the increasing bacterial resistance to antibiotics (Lee *et al*., 2005; Panacek *et al*., 2006). The Ag-NPs interactions with bacteria are dependent on the size and shape of the nanoparticles but bactericide mechanism of Ag-NPs is not clear (Morones *et al*., 2005; Pal *et al*., 2007). The antibacterial activity of the Ag-NPs can be used in several medicine applications for example, to reduce infections in burn treatment (Ulkur *et al*., 2005), dental materials (Ohashi *et al*., 2004) and human skin (Bosetti *et al*., 2002; Gauger *et al*., 2003).

MMT as lamellar clay has intercalation, swelling and ion exchange properties. Its interlayer space has been used for the synthesis of nanoparticles materials (Darroudi *et al*., 2009) and biomaterials, as support for anchoring transition-metal complex catalysts and as adsorbents for cationic ions (Kozak and Domka, 2004). In this research, a wet chemical method to synthesize and antibacterial activity of Ag-NPs using MMT as a solid support is presented. Via this method, we are able to obtain Ag-NPs with different sizes by controlling the percentages of $AgNO_3$ in MMT.

MATERIALS AND METHODS

All reagents were of analytical grades and were used as received without further purification. $AgNO_3$ (99.98%), used as silver precursor was supplied from Merck and Germany. MMT used as a solid support for Ag-NPs, was purchased from Kunipa-F, Japan. $NaBH_4$ (98.5%, Sigma-Aldrich, USA) was used as a reducing agent. All aqueous solutions were prepared with Double Distilled water (DD-water).

Synthesis of Ag/MMT nanocomposites: For the synthesis of Ag/MMT nanocomposites, the silver contents of the samples were 0.5 (S1), 1.0 (S2), 1.5 (S3), 2.0 (S4) and 5.0 g

Corresponding Author: Mansor Bin Ahmad, Department of Chemistry, Faculty of Science, Putra Malaysia University, 43400 Serdang, Selangor, Malaysia

(S5) Ag/100 g MMT. Constant amounts of MMT were suspended in different volumes of 1×10^{-3} M $AgNO_3$ solution and stirred for 24 h. Freshly prepared $NaBH_4$ (4×10^{-2} M) solution was then added to the suspensions under continuous stirring to reach a constant $AgNO_3/NaBH_4$ molar ratio (1:4). After the addition of the reducing agent stirring was continued for another 1 h. The suspensions were finally centrifuged, washed with DD-water twice and dried under vacuum overnight. All experiments were conducted at ambient temperature.

Evolution of antibacterial activity: *In vitro* antibacterial activity of the samples was evaluated by disc diffusion method using Mueller-Hinton Agar (MHA) with determination of inhibition zones in millimeter (mm), which conforms to the recommended standards of the National Committee for Clinical Laboratory Standards (NCCLS). *Escherichia coli* (ATCC 25922), *Staphylococcus aureus* (ATCC 25923), *Klebsiella pneumoniae* (ATCC 13883) and *Escherichia coli* O157:H7 were used for reference of antibacterial effect assay. Briefly, sterile paper discuss (6 mm) impregnated with 20 μL of MMT/Ag nanocomposites (1, 2 and 5% of Ag) suspended in normal saline and were left to dry in 37°C for 24 h in sterile condition. Bacterial suspension prepared by making a saline suspension of isolated colonies selected from an 18-24 h tryptic soy agar plate. The suspension was adjusted to match the tube 0.5 McFarland turbidity standard using spectrophotometer in 600 nm, which equal to 1.5×10^{8} Colony-Forming Units (CFU) mL^{-1}.

The surface of MHA was completely inoculated using sterile swab which steeped in prepared suspension of bacterium. Finally, impregnated discs were placed on the inoculated agar and the petri dish was incubated at 37°C for 24 h. After incubation the diameter of growth inhibition zones were measured. Chloramphenicol (30 μg) and Cefotaxime (30 μg) were used as positive standards in order to control the sensitivity of the bacteria.

Characterization: The Ag/MMT nanocomposites were characterized by Ultraviolet-Visible (UV-vis) spectroscopy, Transmission Electron Microscopy (TEM) and Powder X-Ray Diffraction (PXRD).

The UV-vis spectra were recorded over the range of 300-700 nm by a Lambda 25-Perkin Elmer UV-vis spectrophotometer. TEM observations were carried out on a Hitachi H-7100 electron microscopy and the particle size distributions were determined using the UTHSCSA Image Tool software, Version 3.00 program. The structures of produced Ag/MMT nanocomposites were carried out on a Philips PXRD (X'pert, Cu K_α radiation). The change in interlamellar spacing of MMT and Ag/MMT nanocomposite were also studied by using PXRD in the small angle range of $2°<2\theta<12°$. The PXRD patterns were recorded at a scan speed of 2° min^{-1}. The samples were centrifuged by using high speed centrifuge machine (Avanti J25, Beckman).

RESULTS AND DISCUSSION

The colour of $AgNO_3$/MMT suspensions through reduction process by $NaBH_4$ changed from colourless to light brown, then to brown and finally to green, indicating the formation Ag-NPs in MMT suspension. The stability of synthesized MMT suspensions containing Ag-NPs was found to be stable over a long period of time (>2 months) without any sign of precipitation.

Figure 1 shows the UV-vis absorption spectra of the Ag/MMT suspension as a function of $AgNO_3$ concentration. The characteristic silver Surface Plasmon Resonance (SPR) bands were detected around 400 nm. These absorption bands were assumed to correspond to the Ag-NPs smaller than 10 nm (Aihara *et al*., 1998; Lin *et al*., 2003). While there is no characteristic UV-vis absorption of Ag-NPs before addition of $NaBH_4$ (Fig. 1), growth of the plasmon peak at 396 nm indicates the formation of Ag-NPs in S1 (Fig. 1). Gradual increase in

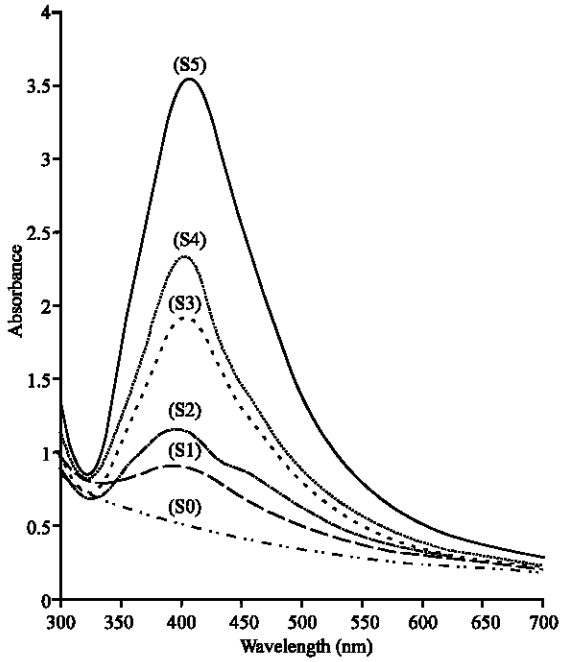

Fig. 1: UV-vis spectra of Ag/MMT suspension as a function of $AgNO_3$ concentration; 0.5% (S1), 1.0% (S2), 1.5% (S3), 2.0% (S4), 5.0% (S5) and $AgNO_3$/MMT suspension in the absence of $NaBH_4$ (S0)

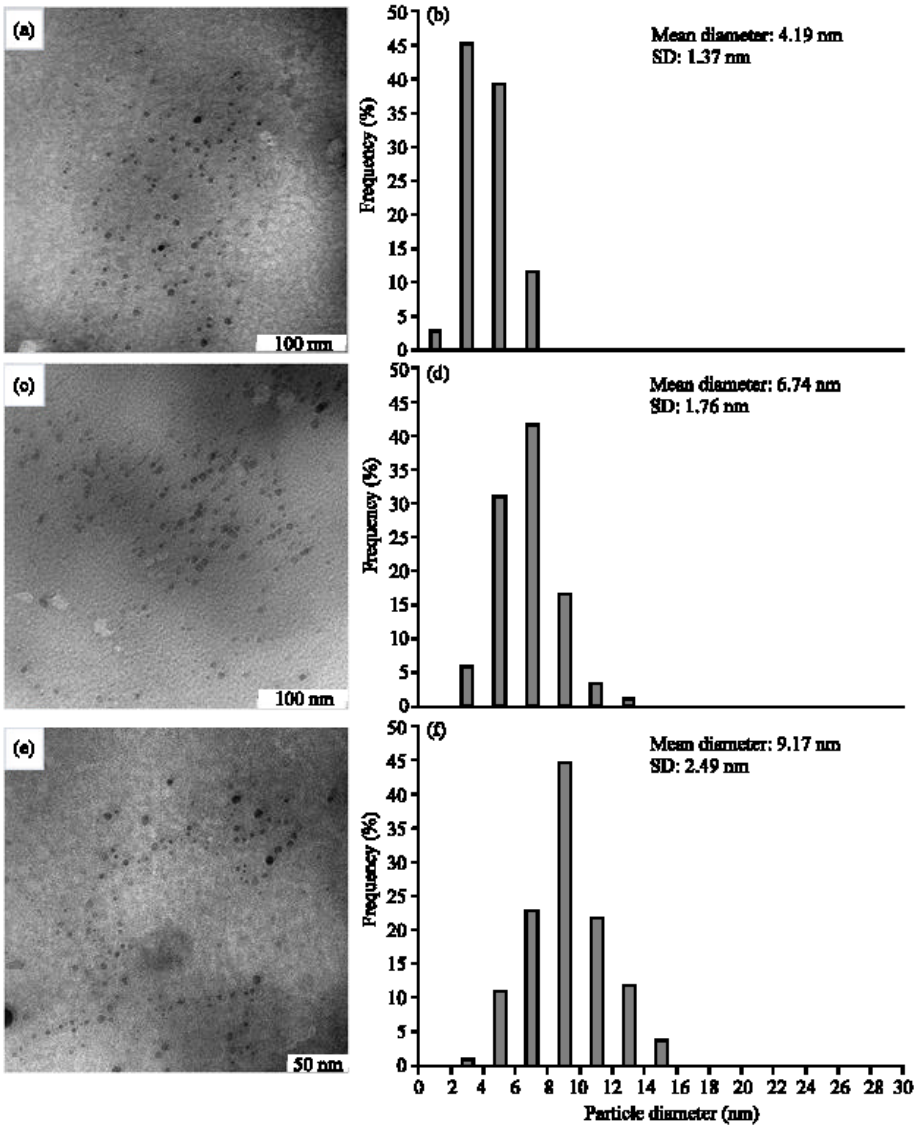

Fig. 2: TEM images and the corresponding particle size distributions of Ag/MMT nanocomposites at different of $AgNO_3$ concentrations ((a-b) 1.0%, (c-d) 2.0% and (e-f) 5.0%)

$AgNO_3$ concentration, from S1-S4, increases the corresponding peak intensities (Fig. 1) in a range of wavelengths from 396-402 nm. In S5, the absorption peak due to SPR of Ag was slightly red-shifted to higher wavelength (404 nm) indicating the increase in the size of Ag-NPs (Liu *et al*., 2007). As shown in Fig. 2a-f, TEM images and their size distributions of synthesized Ag-NPs at different of $AgNO_3$ concentrations, also confirmed this phenomenon.

The comparison between PXRD patterns of MMT and prepared Ag/MMT nanocomposite under chemical reduction route in the small angle range of 2θ ($2° < 2\theta < 12°$) indicates the formation of the intercalated structure (Fig. 3). The original d-spacing (d_L) of MMT, 1.24 nm is increased to 1.30 nm at smaller 2θ angles ($2\theta = 6.79°$ for S4) by silver intercalation. This d_L value is direct proof of the fact that, in the path of ion exchange, Ag^+ ions are bound not only on the external surfaces and edges of MMT but also in the interlamellar space. Metallic nanoparticles formed at the latter location are to cause of the increase in basal spacing. In these samples, the intensities of the reflections are significantly lower whereas their half-widths are larger than those of undoped clay minerals: the highly ordered parallel lamellar structure of the mineral is disrupted by particle formation (Patakfalvi *et al*., 2003).

Table 1: Average of inhibition zones for synthesized Ag/MMT nanocomposites

	Inhibition zone (mm)			Control negative (mm)	Control positive (mm)	
Bacteria	S2	S4	S5	----------MMT----------	Cefotaxime	Chloramphenicol
E. coli	10	9	8	NA*	23	19
S. aureus	8	8	7	NA	28	20
E. coli O157:H7	10	8	7	NA	30	21
K. Pneumoniae	8	7	7	NA	31	25

*Not appear

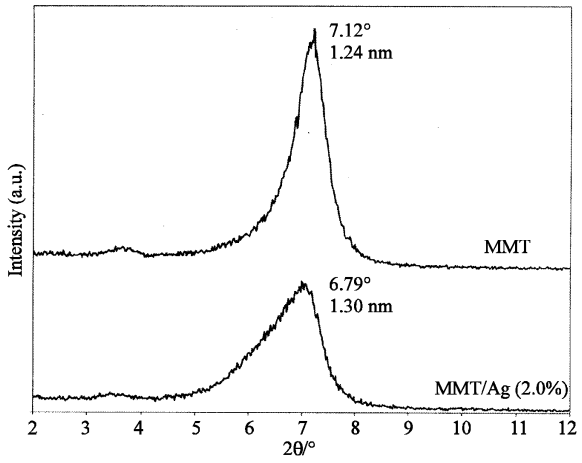

Fig. 3: PXRD patterns of MMT and prepared Ag/MMT nanocomposite for determination of d-spacing (d_L)

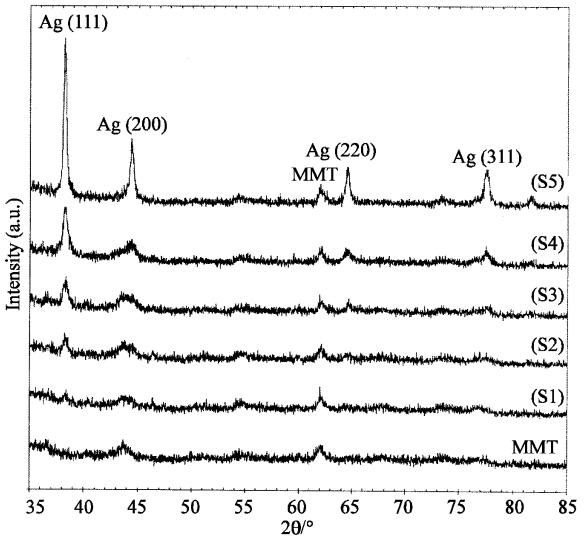

Fig. 4: PXRD patterns of MMT and prepared Ag-NPs into MMT as a substrate at different of $AgNO_3$ concentrations

The PXRD patterns were also employed to determine the crystalline structures of the synthesized Ag-NPs. As shown in Fig. 4, all nanocomposites have similar diffraction profiles and the PXRD peaks at 2θ of 38.28°, 44.38°, 64.52° and 77.61° can be attributed to the (111), (200), (220) and (311) crystallographic planes of face-centered cubic (fcc) silver crystals, respectively (Temgire and Joshi, 2004). For all samples, the main crystalline phase was silver and no obvious other phases as impurities were found in the PXRD patterns. The PXRD peak broadenings of Ag-NPs are mostly due to the presence of nano-sized particles in these nanocomposites (Prasad *et al*., 2006). In addition, there is a characteristic peak in about 2θ = 62.1° that related to MMT (PXRD Ref. #00-003-0010) as a stable substrate.

Inhibition zones values were obtained for the synthesized nanoparticles tested against *Escherichia coli*, *Staphylococcus aureus*, *Klebsiella pneumonia* and *Escherichia coli* O157:H7. The results are presented as average values in Table 1. Table 1 shows that the 4.19 nm Ag-NPs (S2) gives the best antibacterial activity against bacteria. Because of their size, Ag-NPs can easily reach the nuclear content of bacteria and they present the greatest surface area; therefore the contact with bacteria is the greatest (Lok *et al*., 2006). These results show that the antibacterial activity of the nanoparticles varies when their size diminishes.

CONCLUSION

Ag-NPs with different sizes were synthesized in interlayer of MMT in an aqueous chemical reduction method and characterized using TEM, PXRD and UV-vis absorption spectroscopy. The antibacterial activity of the Ag-NPs can be modified with the size of Ag-NPs and it decreases with an increase in the particle size.

REFERENCES

Aihara, N., K. Torigoe and K. Esumi, 1998. Preparation and characterization of gold and silver nanoparticles in layered laponite suspensions. Langmuir, 14: 4945-4949. DOI: 10.1021/la980370p.

Bosetti, M., A. Masse`, E. Tobin and M. Cannas, 2002. Silver coated materials for external fixation devices: *In vitro* biocompatibility and genotoxicity. Biomaterials, 23: 887-892. DOI: 10.1016/S0142-9612(01) 00198-3. PMID: 11771707.

Darroudi, M., M.B. Ahmad, K. Shameli, A.H. Abdullah and N.A. Ibrahim, 2009. Synthesis and characterization of UV-irradiated silver/montmorillonite nanocomposites. Solid State Sci., 11: 1621-1624. DOI: 10.1016/j.solidstatesciences.2009.06.016.

Gauger, A., M. Mempel, A. Schekatz, T. Schafer, J. Ring and D. Abeck, 2003. Silver-coated textiles reduce *Staphylococcus aureus* colonization in patients with atopic eczema. Dermatology, 207: 15-21. DOI: 10.1159/000070935. PMID: 12835542.

Kozak, M. and L.J. Domka, 2004. Adsorption of the quaternary ammonium salts on montmorillonite. J. Phys. Chem. Solids, 65: 441-445. DOI: 10.1016/j.jpcs.2003.09.015s.

Lee, D., R.E. Cohen and M.F. Rubner, 2005. Antibacterial properties of Ag nanoparticle loaded multilayers and formation of magnetically directed antibacterial microparticles. Langmuir, 21: 9651-9659. DOI: 10.1021/la0513306. PMID: 16207049.

Lin, X.Z., X. Teng and H. Yang, 2003. Direct synthesis of narrowly dispersed silver nanoparticles using a single-source precursor. Langmuir, 19: 10081-10085. DOI: 10.1021/la035185c.

Liu, F.K., Y.C. Hsu, M.H. Tsai and T.C. Chu, 2007. Using γ-irradiation to synthesize Ag nanoparticles. Mater Lett., 61: 2402-2405. DOI: 10.1016/j.matlet.2006.07.193.

Lok, C.M., C.M. Ho, R. Chen, Q.Y. He, W.Y. Yu, H. Sun, P.K. Tam, J.F. Chiu and C.M. Che, 2006. Proteomic analysis of the mode of antibacterial action of silver nanoparticles. J. Proteome Res., 5: 916-924. DOI: 10.1021/pr0504079. PMID: 16602699.

Morones, J.R., J.L. Elechiguerra, A. Camacho, K. Holt, J.B. Kouri, J.T. Rami'rez and M.J. Yacaman, 2005. The bactericidal effect of silver nanoparticles. Nanotechnology, 16: 2346-2353. DOI: 10.1088/0957-4484/16/10/059.

Ohashi, S., S. Saku and K. Yamamoto, 2004. Antibacterial activity of silver inorganic agent YDA filler. J. Oral Rehabil., 31: 364-367. DOI: 10.1111/j.1365-2842.2004.01200.x. PMID: 15089943.

Pal, S., Y.K. Tak and J.M. Song, 2007. Does the antibacterial activity of silver nanoparticles depend on the shape of the nanoparticle? A study of the gram-negative bacterium *Escherichia coli*. Appl. Environ. Microbiol., 73: 1712-1720. DOI: 10.1128/AEM.02218-06. PMID: 17261510. PMCID: 1828795.

Panacek, A., L. Kvitek, R. Prucek, M. Kolar, R. Vecerova, N. Pizurova, V.K. Sharma, N. Tatjana and Z. Zboril, 2006. Silver colloid nanoparticles: Synthesis, characterization and their antibacterial activity. J. Phys. Chem. B., 110: 16248-16243. DOI: 10.1021/jp063826h. PMID: 16913750.

Patakfalvi, R., A. Oszko and I. Dekany, 2003. Synthesis and characterization of silver nanoparticle/kaolinite composites. Colloids Surf A., 220: 45-54. DOI: 10.1016/S0927-7757(03)00056-6.

Prasad, V., C.D. Souza, D. Yadav, A.J. Shaikh and N. Vigneshwaran, 2006. Spectroscopic characterization of zinc oxide nanorods synthesized by solid-state reaction. Spect Chim. Acta A., 65: 173-178. DOI: 10.1016/j.saa.2005.10.001.

Temgire, M.K. and S.S. Joshi, 2004. Optical and structural studies of silver nanoparticles. Radiat. Phys. Chem., 71: 1039-1044. DOI: 10.1016/j.radphyschem.2003.10.016.

Ulkur, E., O. Oncul, H. Karagoz, E. Yeniz and B. Celikoz, 2005. Comparison of silver-coated dressing, chlorhexidine acetate 0.5% and fusidic acid 2% for topical antibacterial effect in methicillin-resistant Staphylococci contaminated, full-skin thickness rat burn wounds. Burns, 31: 874-877. DOI: 10.1016/j.burns.2005.05.002. PMID: 16011879.